MESH AND BOUNDARY CONSIDERATIONS IN THE NUMERICAL MODELING OF LARGE 3-D ELECTROMAGNETIC NDT GEOMETRIES

L. Udpa, Y.S. Sun, W. Lord and Y.K. Shin

Department of Electrical Engineering
Colorado State University
Fort Collins, CO 80523

INTRODUCTION

Numerical modeling is particularly useful for simulating the energy/defect interactions associated with electromagnetic methods of nondestructive testing, because of the relative ease with which the awkward boundary conditions and shapes can be handled. With the increasing availablity of commercial code it is worthwhile reminding the potential NDT user of the old computer adage "garbage in, garbage out", as many modeling situations, particularly those associated with large pipeline structures, can present formidable discretization problems in 3D to even the most sophisticated of today's computers, and one must take care in the choice of mesh used for any given problem. This paper describes some situations where mesh choice plays a significant role in the accuracy of numerical code predictions. Two examples considered here, for illustrating these difficulties are (i) the remote field eddy current method and (ii) the flux leakage method, for inspecting ferromagnetic pipelines.

REMOTE FIELD EDDY CURRENT PHENOMENON

The fundamental physical principles governing the remote field eddy current method are the same as those of conventional eddy current method described elsewhere [1,2]. Briefly, conventional eddy current techniques involve the excitation of a coil with an alternating current source and the measurement of changes in the probe coil impedance as the probe scans a test object, which may be a flat surface or a hollow cylinder. A major limitation of the eddy current technique is the skin effect phenomenon [3] which confines the detection to surface or near surface defects. This implies that in the case of tubular conductors, conventional eddy current probes are sensitive largely to I.D. defects. This difficulty is overcome by the remote field eddy current probe which exhibits equal sensitivity to both I.D. and O.D. defects.

The remote field eddy current phenomenon first observed in the 1950's is described in [4]. The significant difference in this technique is that the electromagnetic field of interest is several coil diameters away from the exciter coil as opposed to the conventional eddy current technique where the defect interacts with the field in close proximity to the excitation coil. The geometry of the differential eddy current probe and remote field eddy current probe used in the inspection of a cylindrical tube are shown in Fig. 1.

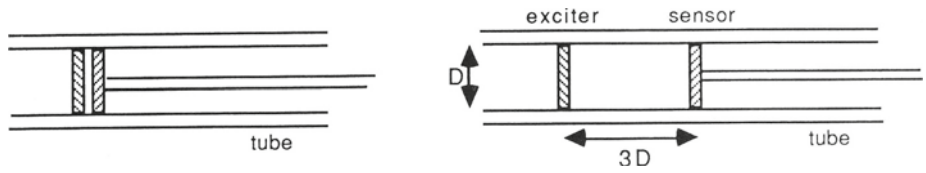

(a) (b)

Fig. 1. The geometry of (a) differential eddy current probe (b) remote field eddy current probe.

Another method that is in use for the inspection of ferromagnetic pipes is based on the magnetic flux leakage principle.

LEAKAGE FIELD PHENOMENON

Active leakage fields can be set up in a ferromagnetic material by simply passing a direct current through it or by applying an external field. The presence of a flaw in the material causes the flux to be redistributed resulting in a local 'leakage' of flux in the vicinity of the defect [5]. The leakage field which is characteristic of the underlying defect, is measured by scanning the surface of the test object with a flux sensitive transducer such as a Hall element probe.

Flux leakage pigs in the form of self contained capsules are used extensively for detecting corrosion in ferromagnetic pipelines. A generic geometry that can be used for modeling this phenomenon is shown in Fig. 2.

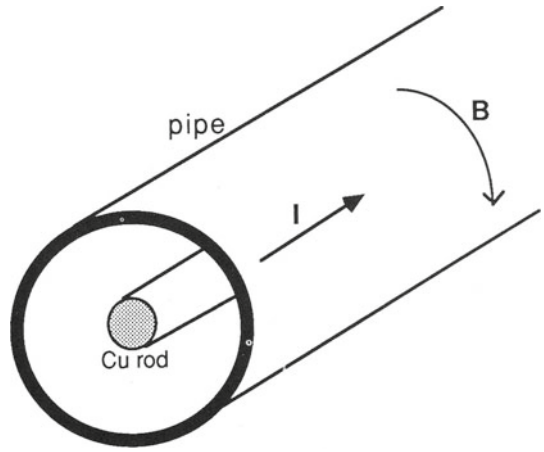

Fig. 2. A generic geometry used for modeling flux leakage method of pipeline inspection.

GOVERNING EQUATIONS

In order to utilize these techniques effectively it is essential to develop a theoretical model to help understand the complex field/defect interactions. Development of analytical models involves the solution of the underlying governing equations, that describes the physics of the process. The governing equations for the leakage flux phenomenon can be derived from the static approximation of Maxwell's equations [7]. In

terms of the vector magnetic potential $\bar{A}$ the governing elliptic equation in three dimensions is

$$\nabla \times \left(\frac{1}{\mu} \nabla \times \bar{A}\right) = \bar{J} \tag{1}$$

where μ is the magnetic permeability and $\bar{J}$ is the excitation current density.

The equations describing the remote field eddy current phenomenon can be obtained using the quasistatic approximation of the Maxwell's equations [3] as

$$\nabla \times \left(\frac{1}{\mu} \nabla \times \bar{A}\right) = \bar{J} - j \omega \sigma \bar{A} \tag{2}$$

where σ is the electrical conductivity and ω is the frequency of the steady state excitation current.

As in most engineering applications, Eqns. (1) and (2) can be solved analytically in one dimension and maybe for some simple two dimensional geometries [7,8]. But realistic problems involving complex geometries in two and three dimensions can only be solved using numerical techniques. The finite element code developed at Colorado State University has found a variety of modeling applications such as in probe design optimization [11], defect characterization [12] and as a general experimental model for simulating a number of test situations too difficult to replicate in the laboratory.

3D FINITE ELEMENT MODEL

The finite element method does not provide a direct solution to the electromagnetic field Eqs. (1) and (2). Rather this approach, based on principles of variational calculus, minimizes an energy functional derived from the differential equations [11]. The energy functional can in general be expressed as

$$F(\bar{A}) = \int_V (\text{stored energy} - \text{input energy} + \text{dissipated energy})\, dv \tag{3}$$

The solution to the governing equations is obtained by discretizing the three dimensional geometry into hexahedral volumetric elements connected together at a discrete set of nodes, and minimizing the energy functional with respect to the nodal values of the magnetic vector potential. This results in a system of linear equations

$$\frac{\partial F(\bar{A})}{\partial A_{ki}} = 0 \qquad \begin{matrix} i=1,2,3,....N \\ k = x,y,z \end{matrix} \tag{7}$$

where N is the total number of nodes in the region. The set of 3N equations is solved simultaneously for the unknown magnetic vector potential. A more detailed description of the different steps involved, can be found in [12]. However, some important aspects of 3D modeling are discussed next in the context of pipeline inspection using the remote field eddy current and flux leakage methods, described above.

Two major issues that need to be considered in 3D finite element modeling applications are (i) Mesh discretization of domain geometry and (ii) Boundary conditions.

Mesh Discretization

The general rule used in discretization is to use smaller elements in regions of high field gradient and larger elements in regions of low field gradient. One class of problems that can arise at this stage is due to geometry. For example a typical geometry for remote field eddy current inspection of pipes is shown in Fig. 3. A 2 ft. diameter pipe would necessitate a distance of 6-8 ft. between the exciter and sensor coils. Taking into account the boundary effect and edge effects of the pipe [13], an axial distance of 23 pipe diameters or 46 feet, and a radial distance of 11 feet would need to be considered as the domain to be discretized. However for a pipewall thickness of only 0.375 inches, and in order to model defects in the pipe wall with dimension only 10% of the wall thickness, a mesh would be required to accomodate .0375 inch elements. In order to avoid explosive matrix dimensions, axisymmetric mesh structures with large variations in mesh density have been developed [15]. Care was taken to ensure that the mesh did not suffer from numerical instabilities.

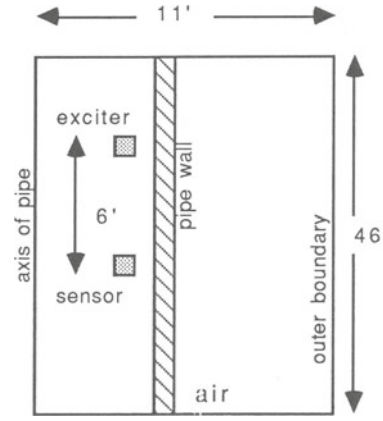

Fig. 3. Typical dimensions encountered in the remote field eddy current inspection of pipelines.

Another class of problems encountered in many applications is due to gradients of the field. In order to optimize the mesh for geometry in Fig. 2, an experimental leakage field defect signal was compared with the corresponding model prediction, using 2D finite element code. Since the gradients of the flux density $\bar{B}$ are large at the pipe wall-air interface (radial direction) and also at the edge of an O.D. slot (circumferential direction), the aspect ratio of the elements in the scanning region immediately above the pipewall is rather critical. The variation of the peak amplitude of the model signal as a function of the aspect ratio of the elements in the scanning layer of the mesh is plotted in Fig. 4. The mesh gave optimum results when the aspect ratio was 1. In other words the dimension of the element in the circumferential direction should be equal to the liftoff measurement (~.005").

When these issues are considered in the context of a 3D mesh, where one has to solve for three components A_x, A_y, A_z at each node, it becomes necessary to exploit possible symmetries of the problem. In order to make the mesh small enough for the CYBER 205 Supercomputer at Colorado State University, only one quadrant of actual geometries was modeled by the 3D finite element code, assuming symmetry about the xy and yz planes as shown in Fig. 5. However, this leads to errors in the specification of boundary conditions on the different sides, of the three dimensional region.

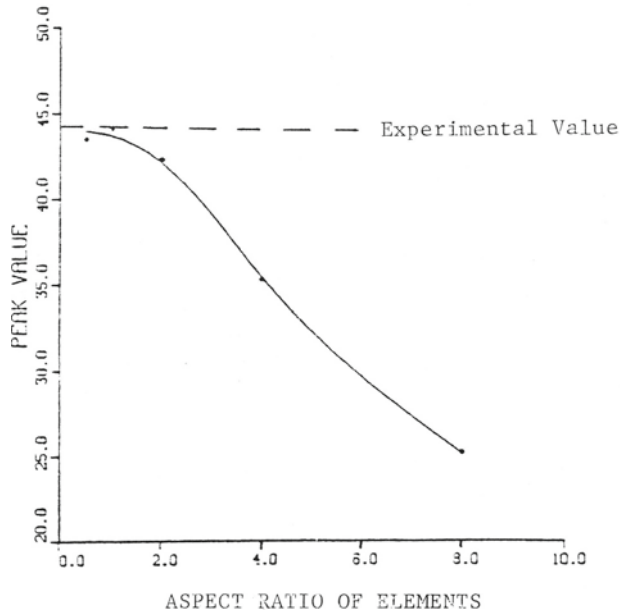

Fig. 4. Variations of the peak amplitude of the flux leakage defect signals with aspect ratio of the elements in the scanning region.

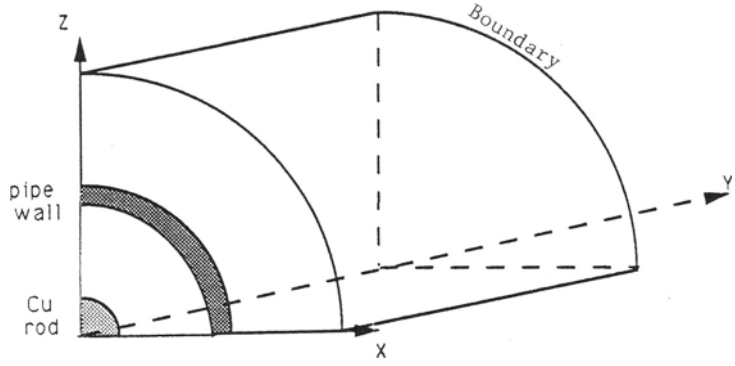

Fig. 5. One quadrant of the geometry in Fig. 2, used in 3D finite element model.

Boundary Conditions

Consider the case of the one quadrant leakage field geometry in Fig. 5. The outer boundary 'bcef' is placed far enough apart so that the gradient of A at these boundaries is negligible. The Dirichlet boundary conditions as shown were imposed on side bcef. However the boundary conditions on all three components of the magnetic vector potential are not known on the xy and yz planes, in the presence of a three dimensional defect. The boundary conditions in the absence of a defect were calculated as shown in Fig. 6 and the same conditions were assumed to be valid in the presence of defects. However, under certain conditions of defect size the error introduced by these boundary conditions becomes comparable to the signal strength. Fig. 7 shows the results for the radial and circumferential component, B_r and B_θ for a defect free situation and the variations of B_r for an infinitely long defect is shown in Fig. 8. Since the boundary conditions used are valid for both these situations the results were good. However when a three dimensional slot of length = 0.5", depth = 0.05" and width = .2" was introduced in the pipe wall, the boundary conditions are no longer valid and introduce an error in the solution as seen in Fig. 9. In order to avoid these problems a full geometry mesh is required but this would result in an extremely large mesh and matrix size, calling for significantly larger computer resources.

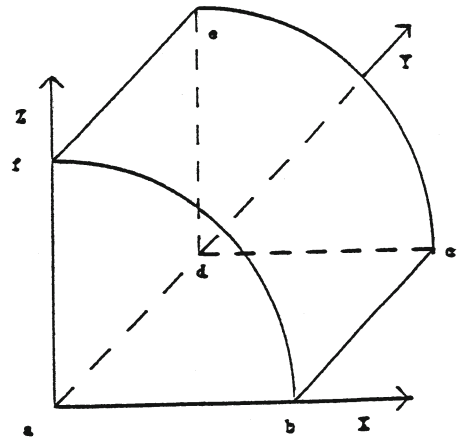

On abcd :	**Az = 0 ; Ax, Ay floating**
On adef:	**Ax = 0 ; Ay, Az floating**
On abf, dce:	**Az = Ax = 0 ; Ay floating**
On bcef:	**Ax = Ay = Az = 0**

Fig. 6. Boundary conditions on the planes of symmetry for the defect free geometry.

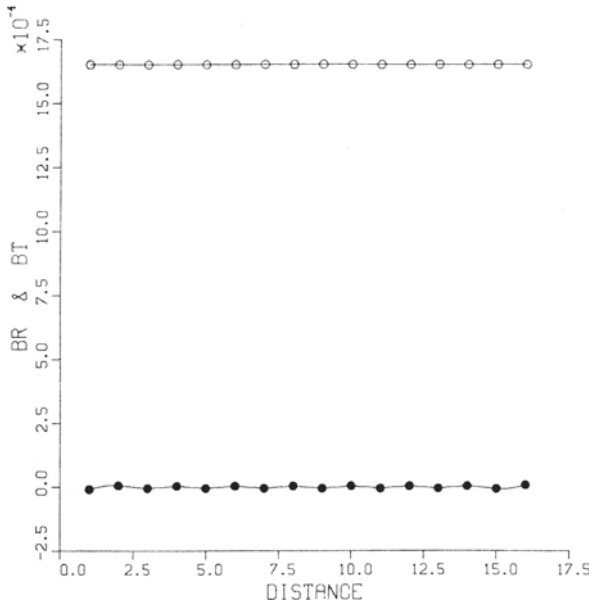

Fig. 7. Radial and circumferential components of flux density on the outer surface of the pipe, for a defect free situation (2D geometry).

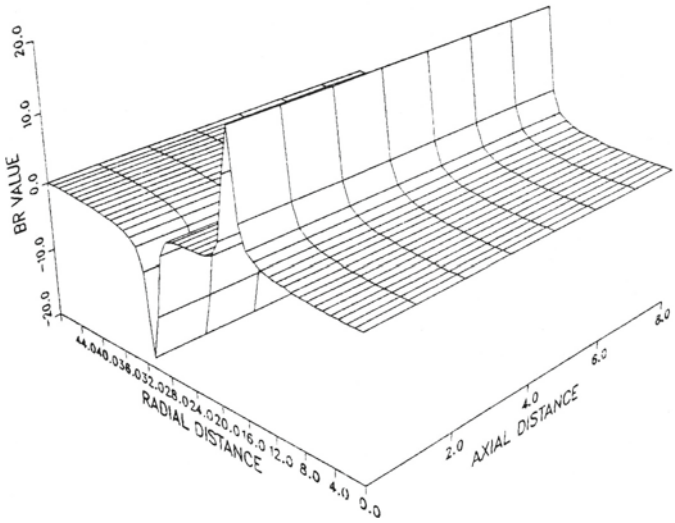

Fig. 8. Leakage field profile for an infinitely long defect (2D geometry) showing validity of the boundary condition in Fig. 6.

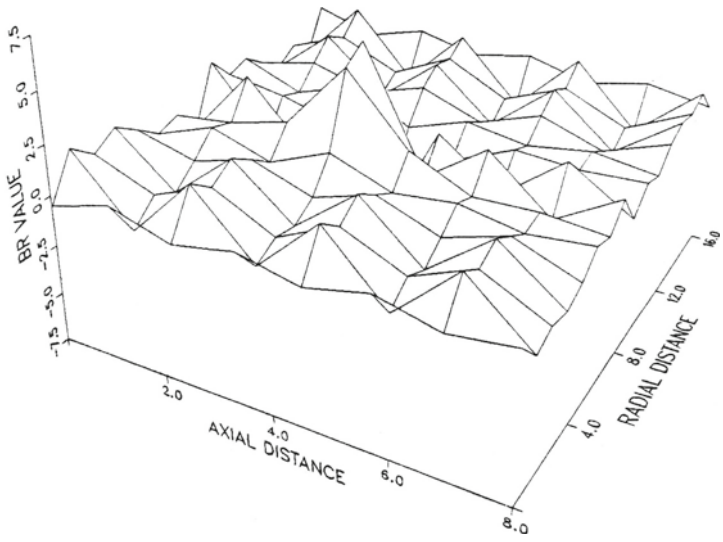

Fig. 9 Leakage field profile due to a three dimensional rectangular slot on the outer surface of pipe wall, showing the error introduced by invalid boundary conditions.

CONCLUSIONS

The extension of existing 2-D numerical NDT modeling codes to 3-D is fraught with difficulties, not the least of which is the need to handle large, intricately-shaped testing geometries containing relatively small defect shapes. This paper describes two situations in which the choice of mesh and boundary conditions plays a critical role in the accuracy of code predictions, and emphasizes again the need for careful experimental confirmation of any numerical results.

REFERENCES

1. H.L. Libby, Introduction to Electromagnetic Nondestructive Test Methods (Krieger Publishing Co., New York, 1979).
2. M.L. Burrows, Ph.D. Dissertation, University of Michigan, 1964.
3. R. Palanisamy, Ph.D. Dissertation, Colorado State University, 1980.
4. T.R. Schmidt, Materials Evaluation, Vol. 42, February 1984, pp. 225-230.
5. H. Luz, Nondestructive Testing, Vol. 6, No. 1, February 1973, pp. 8-24.
6. J.H. Hwang, Ph.D. Dissertation, Colorado State University, 1975.
7. C.V. Dodd, Ph.D. Dissertation, University of Tennessee, June 1967.
8. D.H.S. Cheng, Ph.D. Dissertation, University of Missouri, 1964.
9. S.R. Satish and W. Lord, in Review of Progress in Quantitative Nondestructive Evaluation, edited by D.O. Thompson and D.E. Chimenti (Plenum Press, New York, 1982), Vol. 1, pp. 79-81.
10. W. Lord and J.H. Hwang, Brit. J. NDT., Vol. 19, No. 1, January 1977, pp. 14-18.
11. O.C. Zienkiewicz, The Finite Element Model (McGraw Hill Book Company, London, 1977).
12. N. Ida, Ph.D. Dissertation, Colorado State University, 1983.
13. S. Nath, M.S. Thesis, Colorado State University, 1988.